

THE DISCOVERY OF SPIRAL ARMS IN THE STARBURST GALAXY M82

Y. D. MAYYA, L. CARRASCO, AND A. LUNA

Instituto Nacional de Astrofísica, Óptica, y Electrónica, Luis Enrique Erro 1, Tonantzintla, C.P. 72840, Puebla, Mexico;
ydm@inaoep.mx, carrasco@inaoep.mx, aluna@inaoep.mx

Received 2005 April 8; accepted 2005 June 10; published 2005 July 6

ABSTRACT

We report the discovery of two symmetric spiral arms in the near-infrared (NIR) images of the starburst galaxy M82. The spiral arms are recovered when an axisymmetric exponential disk is subtracted from the NIR images. The arms emerge from the ends of the NIR bar and can be traced up to 3 disk scale lengths. The winding of the arms is consistent with an $m = 2$ logarithmic spiral mode of pitch angle 14° . The arms are bluer than the disk in spite of their detection on the NIR images. If the northern side of the galaxy is nearer to us, as is normally assumed, the observed sense of rotation implies trailing arms. The nearly edge-on orientation, high disk surface brightness, and presence of a complex network of dusty filaments in the optical images are responsible for the lack of detection of the arms in previous studies.

Subject headings: galaxies: individual (M82) — galaxies: starburst — galaxies: structure

Online material: color figures

1. INTRODUCTION

M82 is a nearby edge-on galaxy ($D = 3.63$ Mpc, image scale 17.6 pc arcsec $^{-1}$; Freedman et al. 1994) that has revealed interesting phenomena at every spatial scale investigated; on the largest scale, a bridge of intergalactic gas, spanning over 20 kpc, connects M82 with its neighbor M81 (Gottesman & Weliachew 1977). The external part of the stellar disk (radius ~ 5 kpc) is warped in the direction of the H I streamers detected by Yun et al. (1993). The central 500 pc of the galaxy harbors a starburst, the prototype for the starburst phenomenon (Rieke et al. 1980). Starburst-driven galactic superwinds were detected up to distances of 10 kpc above the plane of the galaxy (Lehnert et al. 1999). Surrounding the active starburst region, there are a molecular ring of 400 pc radius (Shen & Lo 1995) and a near-infrared (NIR) bar of ~ 1 kpc length (Telesco et al. 1991). A network of dusty filaments dominates the optical appearance of the galaxy. Morphologically, M82 belongs to the Irr II class of galaxies (Holmberg 1950), later called I0 by de Vaucouleurs (1959) and “amorphous” by Sandage & Brucato (1979). M82 is a low-mass galaxy ($\sim 10^{10} M_\odot$), with most of its mass concentrated within the central 2 kpc (Sofue 1998).

There is overwhelming evidence that M82 has recently undergone close encounters with its massive neighbor M81 and the dwarf galaxy NGC 3077 (Yun et al. 1994). Detailed N -body simulations of interacting systems have shown that the onset of gaseous infall is intimately related to the formation of global bars and/or spiral arms (i.e., $m = 2$ mode), which help drive the gas toward the central regions (Toomre & Toomre 1972; Barne & Hernquist 1992; Mihos 1999). The presence of the NIR bar in M82 is in agreement with this general picture. However, in M82 the bar occupies only 1/10 of the optical disk, suggesting that there may be hidden components such as spiral arms extending over the entire disk. Given the large amount of extinction in the optical bands, a careful analysis of NIR images is needed to uncover such features. Ichikawa et al. (1995) carried out NIR surface photometry of M82 and found distortions in the isophotes outside the central bar, which they assumed to be related to the warp of the external disk. In this Letter, using new deep NIR images, we comprehensively show that these isophotal distortions in M82 are due to the presence of a two-armed logarithmic spiral structure.

In § 2 we describe the observations and the techniques adopted in their analysis. In §§ 3 and 4 we characterize the properties of the disk and spiral arms. Finally, in § 5 we discuss the morphological type of M82.

2. NEW NIR OBSERVATIONS AND ANALYSIS

New NIR imaging of M82 in the J , H , and K bands was obtained during 2004 March 30 and 31 with the CANanea Near Infrared Camera (CANICA) available at the 2.1 m telescope of the Observatorio Astrofísico Guillermo Haro in Cananea, Sonora. CANICA hosts a 1024×1024 format HAWAII array. The image scale and field of view of the camera are $0''.32$ pixel $^{-1}$ and $\sim 5'.5 \times 5'.5$, respectively. A sequence of object and sky images was taken, with the final co-added images corresponding to integration times on the object of 18, 6, and 12.5 minutes in the J , H , and K bands, respectively. The FWHM of the seeing disk was $\sim 2''.5$. The galaxy slightly overfills the detector array, and the outermost isophotes in our images correspond to surface brightness levels of 19.5 ± 0.1 , 19.0 ± 0.3 , and 18.5 ± 0.2 mag arcsec $^{-2}$ in the J , H , and K bands, respectively. The signal-to-noise ratio is in excess of 50 for the azimuthally averaged intensities. Photometric standard stars from Hunt et al. (1998) were observed to calibrate the images. The resulting magnitudes for the central $35''$ aperture agree within 0.05 mag with those extracted over the same aperture from the 2MASS archival images. Further information on the CANICA instrumentation and the reduction package can be found in L. Carrasco et al. (2005, in preparation).¹ We complemented our NIR data with B -band images (Marcum et al. 2001), archived at the NASA Extragalactic Database (NED).

3. SURFACE PHOTOMETRIC ANALYSIS

The optical appearance of M82 is dominated by bright star-forming knots interspersed by the dusty filaments. However, in the NIR the light distribution is smooth, rendering the images ideal for studying the properties of the stellar disk. Ichikawa et al. (1995) analyzed NIR images and found variations of the position angle (P.A.) of the semimajor axis and

¹ See <http://www.inaoep.mx/~astrofi/cananea/canica>.

axial ratio b/a as a function of radius. In cases like this, the determination of the inclination of the disk to the line of sight is highly uncertain. Hence Pierce & Tully (1988) have suggested the use of a characteristic b/a value jointly with an intrinsic ratio of the scale height to scale length of 0.20. The range of the observed b/a ratios provides an estimator of error for the inclination angle. For M82, we determine a characteristic $b/a = 0.30$, corresponding to an inclination angle of $77^\circ \pm 3^\circ$. The surface photometry was carried out with the ellipse task in IRAF STSDAS.

We obtained one-dimensional intensity profiles in the J , H , and K bands by azimuthally averaging the intensities in successive annular regions. The one-dimensional intensity profiles in the outer parts of the galaxy follow an exponential law as expected for a stellar disk. A fit to the K -band profile outside a radius of $60''$ yields a scale length of $47'' \pm 3''$ (825 ± 50 pc), in good agreement with the values obtained by Ichikawa et al. (1995). The error on the scale length was estimated by fitting an exponential function to different one-dimensional profiles, each profile obtained by varying b/a between 0.28 and 0.32 and P.A. between 62° and 65° . The scale lengths in the J and H bands are identical to that in the K band within the quoted errors.

3.1. The Azimuthal Structure and the Spiral Arms

An image of the M82 disk was constructed from the exponential scale length and the ellipse-fitting parameters. This was subtracted from the observed JHK -band images in order to obtain three residual images. Nonaxisymmetric structures such as a bar and spiral arms are expected to stand out on these images. A combined image of these residual images is displayed in Figure 1a. The most prominent component in this image is a bright linear structure of $120''$ length centered around the nucleus, which then extends as arcs out to a radius of $\sim 160''$. The bar discovered by Telesco et al. (1991) occupies only the central $60''$. The rest of the linear structure, along with the arcs, represents spiral arm structure viewed almost edge-on, as we demonstrate below. The K -band residual image contours are superposed on a B -band image in Figure 1b. Note that the spiral arms are not seen directly in the B band. However, all the bright blue knots lie along our spiral arms.

The most common technique adopted to characterize the properties of the spiral arms is to analyze the azimuthal intensity profiles on deprojected images using Fourier analysis. For galaxies with large inclinations, as is the case for M82, the face-on view of the galaxy cannot be recovered by deprojection. Hence, we followed an alternative approach of projecting models of spiral galaxies to the inferred inclination angle for M82 and comparing the azimuthal profiles of these images with those in the K band. A face-on model of M82 is constructed by adding the light of an $m = 2$ spiral mode of a given pitch angle to that of an exponential disk. Details of this model are given in § 4.

The observed azimuthal profiles are compared with model profiles in Figure 2a, where azimuthal profiles for radii in the $40''$ to $160''$ range are plotted. The largest plotted radius corresponds to 3.4 times the disk scale length. The northeastern and southwestern arms are easily noticeable at P.A.'s of 65° and 245° , respectively. As expected for a logarithmic spiral, the azimuthal angles of the arms vary systematically with radius. In our case, the azimuthal angle turns over at $\approx 80''$ radius. The plotted profiles for the $m = 2$ model illustrate that this

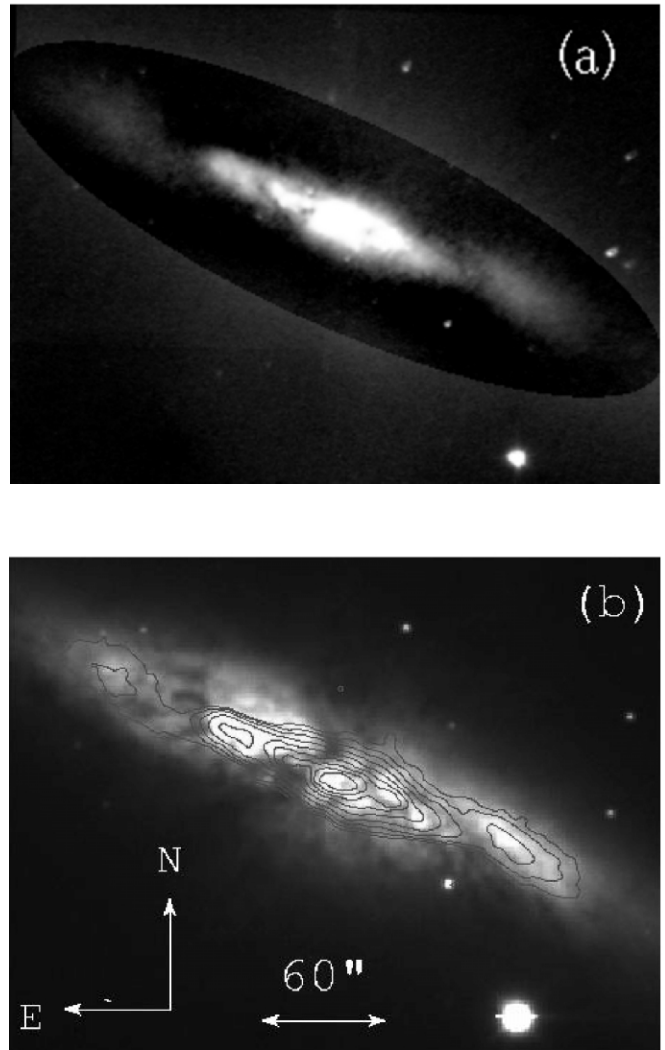


FIG. 1.—(a) Gray-scale representation of the NIR residual image, obtained by subtracting an exponential disk from the observed JHK images. The central bright $60''$ corresponds to the bar, with the outer structures suggesting the presence of a two-armed spiral mode. (b) The contours of the K -band residual image are superposed on a B -band image. Note that most of the B -band knots lie on the spiral arms. A prominent dust lane runs along the inner arc of the southwestern arm. The orientation and the image scale are indicated. [See the electronic edition of the *Journal* for a color version of this figure.]

dependence can be traced even in highly inclined systems. The observed azimuthal profiles at various radii are very well reproduced by a two-armed spiral mode with a 14° pitch angle.

The azimuthal profiles are also useful in quantifying the spiral arm contrasts. In the K band, the arms are brighter by about 0.50 ± 0.1 mag with respect to the interarm regions. The corresponding value for the B band is $\approx 1.00 \pm 0.3$ mag. These values translate to contrast parameters $A_K = 1.6 \pm 0.15$ and $A_B = 2.5 \pm 0.7$, following the Elmegreen & Elmegreen (1984) definition, i.e., $A_\lambda = 10^{0.4\Delta m_\lambda}$. These quantities in M82 are a factor of 4 lower than those observed for the grand-design spiral M51.

The azimuthal profiles of the $J - K$ and $B - K$ colors are plotted in Figure 2b. The arms show up as the bluest regions, especially in the $B - K$ color. The southwestern arm is bluer by 1.0 mag in $B - K$ and 0.2 mag in the $J - K$ color. We also find that the location of the largest disk structures detected in near-ultraviolet (2500 \AA) images (Marcum et al. 2001) coincide

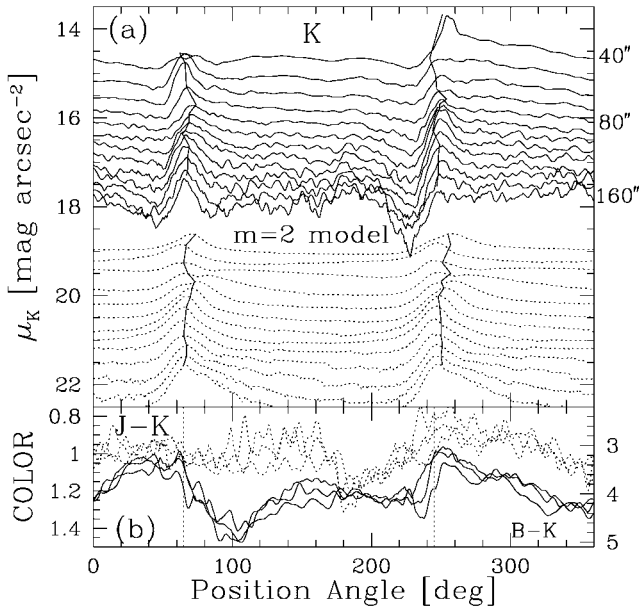


FIG. 2.—(a) Azimuthal intensity profiles in the K -band image compared to an $m = 2$ spiral mode of pitch angle 14° at increasing radial distances between $40''$ and $160''$ at intervals of $10''$. The profiles for the model are shifted downward by 4 mag for clarity. The spiral arms are seen at azimuthal angles of $\sim 65^\circ$ (northeastern arm) and $\sim 245^\circ$ (southwestern arm). Almost vertical solid curves at the position of the arms on the K -band profiles denote the expected radius-azimuth dependence for an $m = 2$ spiral mode. Similarly, the observed radius-azimuth relation is superposed on the model profiles. (b) $J - K$ and $B - K$ (right scale) azimuthal color profiles at three representative radii ($90''$, $110''$, and $130''$). Vertical dotted lines denote the mean position of the spiral arms, where the observed color gradients are the steepest, the arm colors being the bluest. See text for details of the spiral model. [See the electronic edition of the Journal for a color version of this figure.]

with the location of the spiral arms. On the left side of the southwestern arm, the $B - K$ color increases very sharply. This is due to the dust lane present on the concave side of the arm (seen also in Fig. 1b). The azimuth range $65^\circ - 245^\circ$ corresponds to the dustier part of the galaxy, also affected by the superwind cone.

4. THE NATURE AND ORIGIN OF THE SPIRAL ARMS

Why were the spiral arms in M82 overlooked in previous studies in spite of the galaxy's high surface brightness and proximity? The factors that play against an easy detection are (1) the high inclination angle of the disk, (2) the large optical obscuration, and (3) the low contrast of the spiral arms. This combination prevents the detection of the spiral structures even after the advent of NIR detectors. We now investigate the possible nature of the newly discovered arms. Are they trailing in nature as in the majority of galaxies (e.g., de Vaucouleurs 1958)? Do they emerge from the tips of the bar?

In order to answer these questions, we constructed a model galaxy by adding the light of all relevant subcomponents known to exist in M82. The model spiral galaxy contains three main components: an exponential disk, an $m = 2$ mode spiral, and a bar. The $60''$ long bar is tilted with respect to the galaxy major axis by 4° (Telesco et al. 1991). We have adopted such a configuration in our model. A fourth component, a starburst nucleus, modeled as a de Vaucouleurs profile of effective radius $15''$, was also added. The assumed intensity profiles of the bar and the starburst nucleus do not affect our azimuthal profiles,

TABLE 1
PROPERTIES OF GALACTIC SUBCOMPONENTS

Component	Observed	Derived
Inclination (deg)	77 ± 3	76 ± 1
Major-axis P.A. (deg)	62–65	64 ± 1
Disk scale length (arcsec)	47 ± 3	48 ^a
$\mu_K(0)$ (mag arcsec ⁻²)	14.1	15.5 ^a
Bar length (arcsec)	60	60
Spiral ($m = 2$)	Trailing, logarithmic, pitch angle $14^\circ \pm 1^\circ$
Contrast A_K	1.6 ± 0.15	1.20 ^a

^a Face-on values.

since we limit our analysis to radii larger than the bar length. However, the inclusion of the bar in our model helps us to investigate the question of whether or not the spiral arms emanate from their tips. The spiral arms are chosen to be logarithmic in nature and are generated for radii $> 30''$. The intensity along the arms follows the same exponential law of the disk, and hence the contrast of the arms remains constant all along them. Different model galaxies were generated by varying the pitch angle, the initial phase, and the contrast of the spiral arms. The parameters of the model that best reproduce the observed K -band azimuthal intensity profile (i.e., both the observed radius-azimuth and radius-contrast relations for the arms) are chosen as the final ones. The plots for the model in Figure 2a correspond to the best-fit case, whose parameters are listed in Table 1, along with the observed values and errors on them. The errors assigned to model parameters indicate the range over which acceptable fits can be obtained.

The face-on and projected views of the best-matched model galaxy, after subtracting the exponential disk, are displayed in Figure 3. It can be seen that the spiral arms emerge from the ends of the bar,² as is commonly observed in barred galaxies. Arms wind $\sim 360^\circ$ before they can be noticed as such on the residual image at $\sim 80''$ radius. On the projected image, the arms are almost straight features in the $30'' - 60''$ radial zone, appearing as an extension of the bar. The spiral arms are not noticeable unless an exponential disk is subtracted.

The expected sense of rotation of stars in trailing spiral arms is indicated in Figure 3. The observed geometrical and kinematical orientations of the galaxy are also shown. These are based on the scheme adopted by Telesco et al. (1991). This configuration is consistent with the spiral arms being trailing in nature. The presence of a dust lane on the concave side of the southwestern arm also supports the trailing nature of the arms. Besides, the molecular gas distribution in the disk closely follows this dust lane (Walter et al. 2002). Further out, the molecular gas warps, connecting smoothly with the off-planar H I streamers reported by Yun et al. (1993). The joint configuration of the bar, spiral arms, molecular gas, and H I streamers suggests that they are part of a global $m = 2$ mode excited by a close encounter of M82 with its neighbors M81 and NGC 3077. The bisymmetric structure might be facilitating the infall of gas from the debris surrounding M82 all the way to the nuclear region, thus fueling the starburst. In summary, M82 seems to fit well into the picture of spiral formation presented by Toomre & Toomre (1972).

² For the best-fit model with constant pitch angle, shown in Fig. 3, there is a phase difference of $\sim 20^\circ$ between the tips of the bar and the beginning of the arms. However, the arms can be connected to the tips of the bar by allowing the pitch angle to vary smoothly along the arms from 13° in the inner part to 15° at a radius of $160''$.

5. CONCLUDING REMARKS

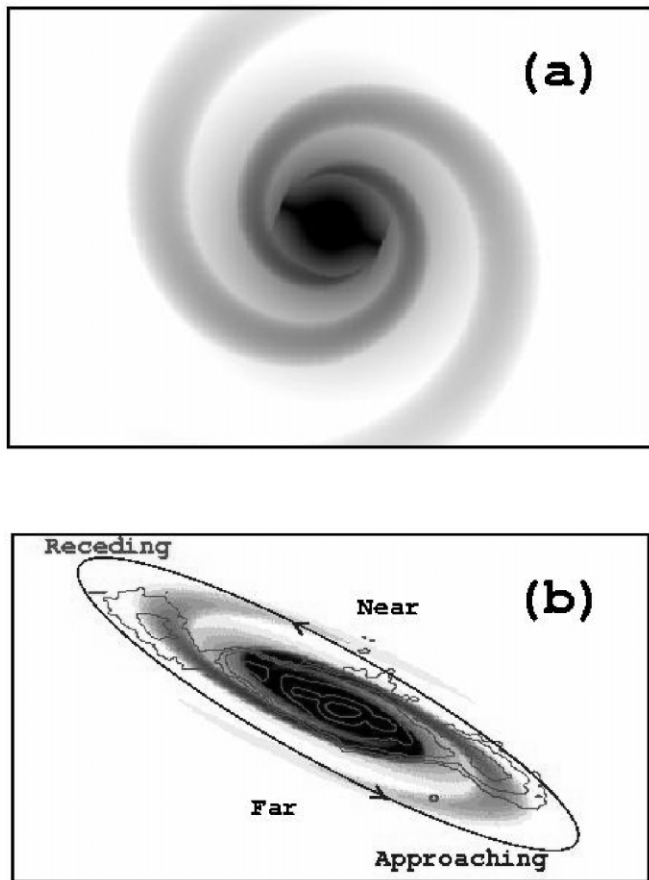


FIG. 3.—Face-on and projected views of the best-matched model galaxy, after subtracting the exponential disk. *K*-band residual image contours are superposed on the latter image. The ellipse with arrows indicates the sense of rotation of stars expected for trailing spiral arms. [See the electronic edition of the *Journal* for a color version of this figure.]

The discovery of spiral arms in M82 throws new light on the inhomogeneous class of galaxies known as Irr II galaxies. These are disk galaxies that differ from spirals in not showing an obvious spiral structure. They differ from irregulars (Im, Sm) by showing a much redder and unresolved disk, and from lenticulars by having an early-type (i.e., younger) stellar spectrum. It is well known that starburst activity, dust obscuration, and tidal interaction play varying degrees of importance in shaping different galaxies in this class (Krienke & Hodge 1974). All the three phenomena are present in M82. In fact, the tidal interaction is responsible for both the chaotic distribution of dust and triggering the starburst activity. This suggests that tidal interaction may play an important role in other galaxies of this class as well. O’Connell & Mangano (1978) have argued that the gross properties of M82—its mass, luminosity, size, and mean spectral type—are comparable to those of normal late-type (Sc/Irr) galaxies. The rather small bulge (mass $\sim 3 \times 10^7 M_{\odot}$; Gaffney et al. 1993) and the relatively open arms inferred in the present work (pitch angle of 14°) suggest a late morphological type SBc for M82.

It is a pleasure to thank A. Bressan, E. Recillas, O. López-Cruz, and I. Puerari for discussions during different phases of this work. The presentation of the paper has vastly improved following the insights given by the referee. We thank G. Escobedo and all the staff at OAGH, especially E. Castillo, for technical help during observations. This work is partly supported by CONACyT (Mexico) research grants G28586-E and 39714-F. This research has made use of the NED, which is operated by the Jet Propulsion Laboratory and NASA.

REFERENCES

- Barne, J. E., & Hernquist, L. 1992, *ARA&A*, 30, 705
 de Vaucouleurs, G. 1958, *ApJ*, 127, 487
 ———. 1959, *Handb. Phys.*, 53, 275
 Elmegreen, B. G., & Elmegreen, D. M. 1984, *ApJS*, 54, 127
 Freedman, W. L., et al. 1994, *ApJ*, 427, 628
 Gaffney, N. I., Lester, D. F., & Telesco, C. M. 1993, *ApJ*, 407, L57
 Gottesman, S. T., & Weliachew, L. 1977, *ApJ*, 211, 47
 Holmberg, E. 1950, *Medd. Lunds Astron. Obs. Ser. II*, 128, 1
 Hunt, L. K., Mannucci, F., Testi, L., Migliorini, S., Stanga, R. M., Baffa, C., Lisi, F., & Vanzi, L. 1998, *AJ*, 115, 2594
 Ichikawa, T., Yanagisawa, K., Itoh, N., Tarusawa, K., van Driel, W., & Ueno, M. 1995, *AJ*, 109, 2038
 Krienke, O. K., & Hodge, P. W. 1974, *AJ*, 79, 1242
 Lehnert, M. D., Heckman, T. M., & Weaver, K. A. 1999, *ApJ*, 523, 575
 Marcum, P. M., et al. 2001, *ApJS*, 132, 129
 Mihos, J. C. 1999, in *IAU Symp. 186, Galaxy Interactions at Low and High Redshift*, ed. J. E. Barnes & D. B. Sanders (Boston: Kluwer), 205
 O’Connell, R. W., & Mangano, J. J. 1978, *ApJ*, 221, 62
 Pierce, M. J., & Tully, R. B. 1988, *ApJ*, 330, 579
 Rieke, G. H., Lebofsky, M. J., Thompson, R. I., Low, F. J., & Tokunaga, A. T. 1980, *ApJ*, 238, 24
 Sandage, A., & Brucato, R. 1979, *AJ*, 84, 472
 Shen, J., & Lo, K. Y. 1995, *ApJ*, 445, L99
 Sofue, Y. 1998, *PASJ*, 50, 227
 Telesco, C. M., Joy, M., Dietz, K., Decher, R., & Campins, H. 1991, *ApJ*, 369, 135
 Toomre, A., & Toomre, J. 1972, *ApJ*, 178, 623
 Walter, F., Weiss, A., & Scoville, N. 2002, *ApJ*, 580, L21
 Yun, M. S., Ho, P. T. P., & Lo, K. Y. 1993, *ApJ*, 411, L17
 ———. 1994, *Nature*, 372, 530